Parameter sensitivity in simulations of snowmelt

Etchevers, Pierre; Essery, Richard

Published in:
Journal of Geophysical Research

Publication date:
2004

Citation for published version (APA):
Etchevers, P., & Essery, R. (2004). Parameter sensitivity in simulations of snowmelt. *Journal of Geophysical Research*.

Parameter sensitivity in simulations of snowmelt

Richard Essery

Centre for Glaciology

Institute of Geography and Earth Sciences

University of Wales, Aberystwyth SY23 3DB

UK

Email: rie@aber.ac.uk

Pierre Etchevers

Centre d'Etudes de la Neige

Météo-France / CNRM

1441 Rue de la Piscine

38406 St Martin d'Heres Cedex

France

Abstract

A simple snow model with only three parameters (fresh snow albedo, albedo decay rate for melting snow and surface roughness) is used to simulate snow accumulation and melt at four sites in Europe and North America, and the extent to which the model's parameters can be calibrated against observations is investigated. Results from the model are compared with observations of snow water equivalent (SWE) and the range of results from models that participated in an intercomparison project for the same sites. Good simulations of SWE are obtained by parameter calibration, but sensitivity analyses show that the SWE observations do not contain enough information to uniquely determine parameter values even for this very simple model. Comparisons of simulated snow albedo with observations for two of the sites give stronger constraints on the model parameters, but the model is unable to give good simulations of SWE and albedo simultaneously with a single parameter set, revealing a weakness due to the model's neglect of internal snowpack processes; an enhanced version of the model representing heat storage in the snow performs better in simultaneous simulations of SWE and albedo. In comparison with observations of snow surface temperature, it is found that sensible heat fluxes in low windspeed conditions have to be enhanced to prevent the model from simulating unrealistically low night-time temperatures at a sheltered site.

1. Introduction

Snowpacks have complex interactions with the overlying atmosphere and

the underlying ground, and the thermal, hydraulic, mechanical and radiative properties of snow can be highly variable in time and space. Models of snowpack processes have been developed for a wide range of applications, including hydrological forecasting, avalanche risk assessment, numerical weather prediction, climate modelling, reconstruction of historical snow records and retrieval of snow characteristics by remote sensing. Different outputs are required from models designed for different applications. Avalanche forecasting requires predictions of the internal structure of a snowpack to allow an assessment of its stability; sophisticated snow physics models have been developed for this application [Brun et al. 1992, Bartelt and Lehning 2002]. To extract information on snow properties from remote measurements of emitted or reflected radiation, models are required that can predict the radiative properties of snow as functions of wavelength, again requiring knowledge of the snow's grain structure [Wiesmann et al. 2000]. In hydrological forecasting, snow models have to predict the timing and magnitude of snowmelt runoff, often in basins for which only limited meteorological data are available [WMO 1986, Hock 2003]; very simple temperature-index models are often used in such applications. Simple models with limited data requirements have also been used in reconstructions of historical snow records for climate studies and evaluation of climate models [Brown and Goodison 1996, Brown et al. 2003]. When implemented as part of a land-surface scheme coupled to an atmospheric model for numerical weather prediction or climate modelling, a snow model has to represent the influences of snow on the albedo of the surface and exchanges of heat and moisture between the surface and the atmosphere.

Accurate simulations of partitioning between sublimation and melt of snow, and timing and rate of snowmelt are also important as these influence soil moisture and hence surface fluxes even after the snow has melted [Yeh et al. 1984, Barnett et al. 1989]. The complexity that can be used in these snow models is constrained by the computational expense of atmospheric models.

Interest in the performance of snow representations in climate models, in particular, has prompted many intercomparisons between models [Frei and Robinson 1998, Essery et al. 1999, Jin et al. 1999, Boone and Etchevers 2001, Bruland et al. 2001, Gustafsson et al. 2001, Frei et al. 2003, Sheffield et al. 2003]. Two phases of the Project for Intercomparison of Land-surface Parametrization Schemes (PILPS) considered sites with seasonal snowcover; PILPS 2d [Slater et al. 2001] compared simulations by 21 models with average snow water equivalent (SWE) from snow courses at a grassland site in Russia, and PILPS 2e [Bowling et al. 2003] compared distributed simulations by 21 models with runoff from a large Scandinavian basin having large variations in vegetation cover. Both studies found a wide range in results from different models. The Snow Model Intercomparison Project (SnowMIP) considered the supposedly simpler problem of simulating SWE at a point for four sites without vegetation or with short vegetation submerged by snow. SnowMIP included both simple and sophisticated models with the aim of providing guidance on the degree of complexity appropriate for specific applications. A wide range was, again, found in the model results [Etchevers et al. 2004].

While intercomparison projects have revealed the range of behaviours

produced by existing land-surface models, a more controlled investigation can be performed using a single model with adjustable parameters or interchangeable process representations; this approach has been used with the Chameleon Surface Model (CHASM) to interpret differences between models in PILPS simulations without snowcover [Desborough 1999, Xia et al. 2002, Jackson et al. 2003] and with snowcover [Leplastrier et al. 2002, Pitman et al. 2003], and Loth and Graf [1998] used a multi-layer snow model to investigate the sensitivity of snow simulations to vertical resolution and the representation of internal processes. In this paper, we use an extremely simple snow surface energy balance model with only three parameters to assess the sensitivity of simulations to variations in these parameters for the SnowMIP sites, and we compare the model sensitivity with the range of results produced by the models that participated in SnowMIP. Meteorological conditions for the winters studied at the four SnowMIP sites are discussed in Section 2, and the energy balance model to be used for the sensitivity studies is described in Section 3. Simulations of SWE by the SnowMIP models, a calibrated degree-day model and the energy balance model are then presented in Section 4. Simulations of albedo and surface temperature by the energy balance model are also discussed for two sites where measurements of these quantities were made.

2. Site characteristics and meteorology

In SnowMIP, hourly records of air temperature, humidity, windspeed, shortwave radiation, longwave radiation, rainfall and snowfall were provided

for complete winters at four sites: Col de Porte (designated CDP here) in the French Alps, Weissfluhjoch (WFJ) in the Swiss Alps, Sleepers River (SLR) in Vermont, USA, and Goose Bay (GSB) in Labrador, Canada. Selected meteorological data (cumulative snowfall, SWE on the ground, windspeed, air temperature and incoming shortwave radiation) for the winters studied in SnowMIP at each site are shown in Figs 1 to 4 and discussed in the following subsections.

2.1 Col de Porte

Col de Porte is a middle elevation site at 1340 m in the French Alps, managed by Météo-France. Snow has been monitored there since 1959. Winter air temperatures are not very low, humidities remain high, windspeeds are low (measurements are made in a forest clearing) and rain can occur at any time during the winter. Data from Col de Porte have been used in many assessments of snow model performance [Brun et al. 1992, Douville et al. 1995, Loth and Graf 1998, Essery et al. 1999, Sun et al. 1999, Strasser et al. 2002, Belair et al. 2003, Xue et al. 2003].

Data from two winters were provided for SnowMIP, but only 1996-1997 will be considered here. Figure 1 shows meteorological and snow data for that winter. SWE was measured weekly in snow pits. The majority of the snowfall occurred in mid to late November. Although there were further snowfalls through the winter, these did not lead to great increases in snow accumulation. The vertical bands in each panel of Fig. 1 highlight periods of ablation revealed by decreases in the measured SWE; there were mid-winter

melt events in December 1996 and January 1997, and the snow finally melted through the course of March.

2.2 Sleepers River

Sleepers River is a middle elevation site at 560 m in northeastern Vermont and has one of the longest historical hydrologic and climatologic databases for a cold region in the United States. The station is in a forest clearing surrounded by a mixed hardwood forest in rolling terrain. The climate is characterized by long, cold winters and cool summers with a mean annual temperature of 6°C. Average annual precipitation is 125 cm, 25% of which falls as snow, with snowcover persisting from early December to mid-April. Prevailing winds are from a westerly direction. The snowmelt model development work of Anderson [1968, 1976] and more recent work by Lynch-Stieglitz [1994] and Albert and Krajeski [1998] used measurements from this site. The site also produced one of six data sets chosen for the World Meteorological Organization's project on Intercomparison of Models of Snowmelt Runoff [WMO, 1986]. Administered by US Army Cold Regions Research and Engineering Laboratory (1979-2002) and the U.S. Geological Survey (1994-present), the location was established by the Agricultural Research Service of the U.S. Department of Agriculture (1958-1975), and for several years was administered by the Office of Hydrology of the National Weather Service (1966-1986).

Data for the winter of 1996-1997 are shown in Fig. 2. SWE was measured on a snow course in a field surrounded by forest; snow accumulated

from late November until the end of March and then melted through April. Although SWE measurements do not show actual decreases before the final melt period, the cumulative snowfall exceeds the accumulation on the ground throughout the winter, suggesting that there was some ablation. Separate measurements of snowfall and rainfall at Sleepers River were not available for SnowMIP. Instead, total precipitation was divided into snow and rain as a linear function of air temperature, with precipitation assumed to be all rain at temperatures above 2°C and all snow below 0°C. This procedure introduces extra uncertainty in the driving data but often has to be adopted in model assessments due to the notorious difficulty of measuring solid precipitation [Goodison et al. 1998].

2.3 Weissfluhjoch

Weissfluhjoch is a high elevation site at 2540 m in the Swiss Alps; the laboratory of the Swiss Federal Institute for Snow and Avalanche Research was established there in 1936. Although the area is windy, the measurement site is sheltered from the dominant northwesterly storms and is not much affected by drifting and blowing snow. The air is cold and dry in winter, but the snowfall is high. In addition to many studies of snow processes, data from Weissfluhjoch have been used in assessments of snow models by Fierz and Lehning [2001], Lehning et al. [2002] and Fierz et al. [2003].

Data for the winter of 1992-1993 are shown in Fig. 3. The SWE measured in snowpits remained close to the cumulative snowfall up until the time of peak accumulation. Snow accumulated and remained dry from late October

until mid-April, and then melted through May and June with high insolation and air temperatures above 0°C.

2.4 Goose Bay

Goose Bay is a low elevation site at 46 m in Labrador, Canada. Meteorological data were collected at the airport there by the Meteorological Service of Canada. Air temperatures are low in winter, but the site is humid and windy. Data from Goose Bay have been used to assess both energy balance and temperature index snow models [Belair et al. 2003, Brown et al. 2003, Xue et al. 2003].

Although data from 15 years were supplied for SnowMIP, only the winter of 1980-1981 is considered here; data for that winter are shown in Fig. 4. The observed SWE was close to the cumulative snowfall until the middle of January, but there was then substantial ablation in February, followed by more accumulation before final melt through April and May. Snow course data were collected in a sparsely wooded area 4 km from the site of the meteorological observations, so these data have to be interpreted with caution. The accumulation of snow following the February ablation highlights the problem of comparing snow models with uncertain driving and evaluation data. The observed SWE increased by 122 mm in March 1981, but only 61 mm of snowfall was recorded over the same period. An accurate simulation of the snowmelt during February would therefore lead to an underestimate in SWE by the end of March. The winter of 1980-1981 is chosen here as an extreme example; discrepancies between measurements of snowfall and snow

accumulation were less marked in other years of record.

3. Model description

The minimal snow model used here is designated MSM for convenience, rather than from any desire to introduce yet another acronym in the field. It performs an energy and mass balance for the surface skin of a snowpack, neglecting all heat and moisture transports within the snow. In common with most of the SnowMIP models, it is driven with hourly averages of incoming shortwave radiation $SW_{\downarrow}$, incoming longwave radiation $LW_{\downarrow}$, air temperature T_1, specific humidity Q_1, windspeed U_1 and snowfall rate S_f. The average surface pressure P_s at a site and the height z_1 above the surface at which the atmospheric measurements were made have to be specified.

Surface radiative and turbulent exchanges are calculated following common procedures used in snow models and land-surface schemes. Surface fluxes of sensible heat and moisture are calculated from

$$H = \rho c_p C_H U_1 (T_s - T_1) \tag{1}$$

and

$$E = \rho C_H U_1 \left[Q_{\rm sat}(T_s, P_s) - Q_1 \right], \tag{2}$$

where ρ and c_p are the density and heat capacity of air, $Q_{\rm sat}(T_s, P_s)$ is the saturation humidity at snow surface temperature T_s and pressure P_s, and C_H is a surface exchange coefficient. The net radiation absorbed by the snow is given by

$$R = (1 - \alpha) SW_{\downarrow} + LW_{\downarrow} - \sigma T_s^4, \tag{3}$$

where α is the snow albedo and σ is the Stefan-Boltzmann constant. Fresh snow is assigned an adjustable albedo α_f. Slow albedo changes for cold snow are neglected, but an exponential decay to an asymptotic minimum of 0.5 with an adjustable time constant τ is applied to melting snow; for each timestep with snowmelt, the albedo is updated according to

$$\alpha \rightarrow (\alpha - 0.5)e^{-\Delta t/\tau} + 0.5, \tag{4}$$

where Δt is the timestep length. For timesteps with snowfall, the albedo is increased by

$$\alpha \rightarrow \alpha + (\alpha_f - \alpha)\frac{S_f \Delta t}{10}, \tag{5}$$

so a 10 mm snowfall refreshes the albedo to α_f.

Atmospheric stability is characterized by the bulk Richardson number

$$\mathrm{Ri_B} = \frac{g z_1}{U_1^2}\left\{\frac{T_1 - T_s}{T_1} + \frac{Q_1 - Q_{\mathrm{sat}}(T_s, P_s)}{Q_1 + \epsilon/(1-\epsilon)}\right\}, \tag{6}$$

where g is the gravitational acceleration and ϵ is the ratio of molecular weights for water and dry air. Following Louis [1979], the exchange coefficient for surface sensible and latent heat fluxes is calculated as $C_H = f_h C_{Hn}$, where

$$C_{Hn} = 0.16\left[\ln\left(\frac{z_1}{z_0}\right)\right]^{-2} \tag{7}$$

is the neutral exchange coefficient for roughness length z_0 and

$$f_h = \begin{cases} (1 + 10\mathrm{Ri_B})^{-1} & \mathrm{Ri_B} \geq 0 \text{ (stable)} \\ 1 - 10\mathrm{Ri_B}(1 + 10C_{Hn}\sqrt{-\mathrm{Ri_B}}/f_z)^{-1} & \mathrm{Ri_B} < 0 \text{ (unstable)} \end{cases} \tag{8}$$

with

$$f_z = \frac{1}{4}\left(\frac{z_0}{z_1}\right)^{1/2}. \tag{9}$$

Scalar and momentum roughness lengths are assumed to be equal; as momentum fluxes are not calculated, and a single reference height is used, any difference is absorbed in the definition of the single roughness length.

Neglecting heat fluxes into the bulk of the snow and heat advected by precipitation, the energy balance of the surface is

$$R = H + L_s E + L_f M, \tag{10}$$

where L_s and L_f are the latent heats of sublimation and fusion, and M is the melt rate. Eqs (1), (2), (3) and (10) form a nonlinear system to be solved for the surface temperature and fluxes at each timestep. To avoid the expense of an iterative solution, the nonlinear terms in T_s are linearized about T_1 and the system is solved algebraically. M is diagnosed as having the value required to prevent the surface temperature exceeding the melting point for snow. The SWE is then incremented by an amount

$$\Delta S = (S_f - E - M)\Delta t. \tag{11}$$

MSM has three adjustable parameters: fresh snow albedo α_f, albedo decay rate for melting snow τ and surface roughness length z_0. This small number of parameters, and the simplicity of the model, allows systematic searches of the parameter space to be made, rather than the Monte-Carlo parameter sampling often used with more sophisticated models and larger parameter sets [e.g. Keesman 1990, Beven and Binley 1992, Jackson et al. 2003].

The influence of heat fluxes into the snow in the energy balance, neglected above, will be investigated with a variant of MSM coupled to the soil and

bulk snow model used in the MOSES land-surface scheme [Cox et al. 1999, Essery et al. 2003]. This has a four-layer soil model representing heat conduction, water movement and phase changes in the top 2 m of soil. The snowpack is represented as a modification of the surface soil layer. As a one-layer, composite snowpack model, this model variant is designated MSM1c following the classification of Slater et al. [2001]. Internal processes of water storage and freezing in the snowpack are still neglected. New parameters are introduced for the density and thermal conductivity of snow. These could be taken as adjustable or parametrized; several models include empirical representations of snow densification and calculate thermal conductivity as a function of density [e.g. Verseghy 1991, Douville et al. 1995]. Instead, these parameters are assigned fixed values here: 250 kg m^{-3} for density and 0.265 $Wm^{-1}K^{-1}$ for conductivity.

4. Simulation results

4.1 SWE simulations

The SWE observations for each site are reproduced again in Fig. 5. The grey bands in this diagram show the envelopes of SWE simulations by the SnowMIP models, excluding two outliers that may have had problems with the specification of snowfall. There is generally a small range between the models while the observed SWE remains close to the cumulative snowfall, but a wide spread develops between simulations once the snow begins to ablate. Most of the models overestimate the accumulation for SLR and GSB. Maximum, minimum and average rms errors in simulated SWE, normalized

by the standard deviations of the observations shown in Fig. 5 for each site, are given in Table 1. These measures show a wide range between models, and the best simulation was given by a different model for each site.

Before turning to the energy balance model MSM, Fig. 5 also shows the performance of a temperature index model (dotted lines). Melt is calculated by multiplying positive degree days by a calibrated melt factor chosen to minimize the rms error in SWE for each site separately; this factor ranges from 1.1 mm $^{\circ}C^{-1}day^{-1}$ for CDP to 5.7 mm $^{\circ}C^{-1}day^{-1}$ for GSB, similar to values obtained in previous studies reviewed by Hock [2003]. For SLR and GSB, the temperature index model gives results that lie well within the range of the SnowMIP results. For the alpine sites CDP and WFJ, however, this model underestimates the peak accumulation and overestimates the duration of snowcover. Better results can be obtained for these sites using an extended temperature index model with a melt factor that increases with the age of the snow and a calibrated temperature threshold for melting [Ross Brown personal communication, Brown et al. 2003].

MSM was first run for each site using the default parameters in Table 2. The resulting SWE simulations are shown by dashed lines on Fig. 5. Snowcover duration was well simulated for all sites, but peak SWE was overestimated for SLR and GSB, and the winter ablation at GSB in February 1981 was not captured (although, as discussed in Section 2, the observations have to be interpreted with caution due to the distance between the snowfall and SWE measurement sites). Normalized errors for these simulations are given in Table 1; the MSM default parameters give good results in compari-

son with the SnowMIP averages for all sites. The model was then calibrated by adjusting its parameters to minimize the rms error in the SWE simulation for each site, giving the results shown by solid lines on Fig. 5 and errors quoted in Table 1 for the site-specific parameters given in Table 2. Calibration substantially reduces the rms errors for all sites. Improved simulations for SLR and GSB are largely achieved by increasing the surface roughness to increase downward sensible heat fluxes and induce some midwinter melting, reducing the peak snow accumulation, while increasing the albedo to prevent early melting in the spring; indeed, the calibrated albedos for SLR and GSB, and roughness lengths for SLR and WFJ, are higher than might be expected for snow. Errors and parameters obtained by minimizing the sum of the normalized errors for all sites are also given in Tables 1 and 2; this calibration for a single parameter set only gives a moderate improvement in performance over the default parameter set (and, in fact, no improvement for SLR).

The ability to produce reasonable simulations of SWE at all four SnowMIP sites with a very simple snow model is no great achievement; this was done by calibration of model parameters against observations that were not available to the SnowMIP participants. What is of more interest is how sensitive the MSM simulations are to changes in the model parameters. Figure 6 shows how the rms error in the SWE simulations change as each of the three MSM model parameters are varied while the others are held at their calibrated values. For α_f, too high a value gives too late a melt and too low a value gives too early a melt, so there is some intermediate value that minimizes the rms error. For τ and z_0 there are clearly poor choices, but there are also ranges

of these parameters to which the rms error is not sensitive; this occurs if the albedo decay time is made large compared with the time between snowfalls that reset the albedo to α_f or if the surface roughness is made small enough that turbulent heat fluxes are negligible.

By plotting contours of rms error, the influence of two parameters on a simulation can be shown at once. This is illustrated in Fig. 7 for variations in α_f and τ, and Fig. 8 for α_f and z_0. In each case the region of the parameter space giving minimum errors is shaded. In these plots, contours running parallel to a parameter axis show a simulation to be insensitive to that parameter; the near-vertical contours for CDP in Fig. 8, for example, show that the simulation is fairly insensitive to the roughness length for values less than 10^{-2} m at this site. Any slope in the shaded region, however, shows that there are different parameter choices that give equally good simulations - α_f and τ for CDP, or α_f and z_0 for WFJ, for example - and the SWE records do not contain enough information to determine the parameters independently. This has been termed equifinality in hydrological modelling [Beven and Binley 1992] but is a common problem for fitting model parameters to limited data [Dyson 2004]. The shaded regions in Fig. 7 all slope down towards the right (high α_f and low τ) to some extent because an increase in melt due to faster albedo decay can be offset by a higher initial albedo. Fitting a curve through the shaded region on Fig. 7 for CDP, for example, shows that very similar simulations can be obtained for any value of α_f between 0.85 and 0.95 with $\tau \approx 83\alpha_f^{-7.6}$. In Fig. 8, the shaded regions slope up towards the right as the balance shifts between the contributions of net shortwave radiation (low

albedo) and sensible heat flux (high roughness) in the simulated snowmelt.

4.2 Albedo simulations

Reflected shortwave radiation over snow was measured at CDP and WFJ, so it is possible to calculate the snow albedo for these sites, although there is some concern that the CDP albedo is underestimated due to surfaces other than snow in the sensor's field of view [Etchevers et al. 2004]. The solid lines on Fig. 9 show effective albedos calculated by dividing total daily outgoing by total daily incoming shortwave radiation measurements. At CDP the albedo showed large variations as the snow repeatedly started melting and was then covered by fresh snow throughout the winter, whereas the albedo at WFJ remained high through the cold winter but dropped rapidly with the start of melt in mid-April.

Optimizing the parameters of MSM to minimize rms errors in albedo simulations gives results shown by dashed lines on Fig. 9. Albedo decay for melting snow is simulated quite well for both sites. The decay in albedo for cold snow between snowfall events seen at WFJ is not reproduced by MSM but can be well-represented by models that include this process [Etchevers et al. 2004]. Unfortunately, the MSM parameters that gave the best simulations of SWE do not give good simulations of albedo; the dotted lines on Fig. 9 show that these parameters give overestimates of the albedo. The inability of MSM to accurately simulate SWE and albedo simultaneously is illustrated in Fig. 10, which shows contour plots of rms errors in albedo simulations for CDP and WFJ as the parameters α_f and τ are varied; the regions of

the parameter space giving minimum albedo errors do not overlap with the regions giving minimum SWE errors (the shaded regions from Fig. 7 are reproduced on Fig. 10 for comparison). MSM does, however, give well-defined minima in the rms errors for albedo simulations. As the model has to match both the high albedo of fresh snow and the albedo decay rate of melting snow, timeseries of albedo measurements contain enough information to determine site and model specific values for these parameters without equifinality.

It is not surprising that a good simulation of SWE with MSM gives an overestimate of albedo, because MSM neglects internal processes of heat and water storage that delay melt; the excess energy that goes into snowmelt as a result can be compensated by increasing the albedo to reduce the net shortwave radiation. MSM1c does, however, include the energy required to warm snow to 0°C before melting begins in its surface energy balance. Figure 11 shows the same results as Fig. 10 but from MSM1c simulations. The inclusion of heat storage in the snow has little influence on the rms errors in albedo for particular choices of α_f and τ, but the region of the parameter space giving minimum SWE errors is shifted to lower albedos, making better compromises between the objectives of minimizing errors in SWE and albedo simulations possible. The change in model formulation has a much bigger influence for CDP than for WFJ; the higher windspeeds at WFJ increase the turbulent heat fluxes into the snow, so some of the extra energy required for snowmelt in MSM1c can be supplied by turbulent fluxes, whereas MSM1c simulates low turbulent fluxes for the low windspeeds at CDP and the extra

energy has to be supplied by decreasing the albedo to increase the input of net shortwave radiation.

When the parameters of an imperfect model are calibrated by comparison with uncertain measurements of more than one predicted quantity, it is likely that it will not be possible to minimize all of the objective functions simultaneously. The problem of many parameter sets giving equally good simulations of one quantity is then replaced by the problem that optimal simulations of different quantities are given by different parameter sets. Indeed, Gupta et al. [1998] argued that the calibration problem is inherently multi-criterion even for assessment against timeseries of a single quantity because many different objective functions can be defined (e.g. rms error, average error and error in duration of snowcover for SWE simulations) and some of them may be independent. Rather than identifying the unique choice of parameters that minimizes a single objective function, Gupta et al. [1998] define the "Pareto set" of parameter choices for multiobjective optimization. From simulations spanning the parameter space, the Pareto set is determined by rejecting those parameter values for which there exists another choice that gives a simulation with lower values for all the objective functions. Plotting the values of two objective functions, such as the rms errors in SWE and albedo considered here, for the parameter choices in the Pareto set gives a curve. Pareto curves for WFJ and CDP albedo and SWE simulations are shown in Fig. 12 for simulations using MSM (dashed lines) and MSM1c (solid lines). Nearly horizontal and vertical parts at the ends of these curves show equifinality in albedo and SWE simulations: a range of parameter values that

gives different errors in the simulation of one quantity but little difference in the simulation of the other. Sloping parts of the curve show that there is some compromise between the quality of albedo and SWE simulations; if a single parameter set gave optimal simulations for both quantities simultaneously, the Pareto curve would be a point. The asymptotes approached by the MSM and MSM1c Pareto curves are quite similar, so the best simulations of either SWE or albedo alone attainable by the two models are similar (this could be because of remaining inadequacies in the model structure, such as the neglect of processes changing the albedo of cold snow, but uncertainties in the observations used for driving and evaluating models will limit the performance that can be achieved with even a perfect model). Because the MSM1c curves are shorter, however, the parameters giving the best SWE simulations give better albedo simulations, and vice versa, with MSM1c than MSM. Moreover, because the MSM1c curves lie below the MSM curves, particularly for CDP, there is less compromise between the quality of the SWE and albedo simulations with MSM1c. The numbers of members in the Pareto sets, and hence the volumes of the parameter space that they span, are reduced in MSM1c compared with MSM - only by 9% for WFJ but by 48% for CDP - so a more robust calibration is possible for MSM1c. Similarly, Xia et al. [2002] found that the most complex mode of the CHASM model could be calibrated more accurately and gave a smaller parameter range for simulations of net radiation, sensible heat flux and latent heat flux than simpler modes with the same number of parameters.

4.3 Surface temperature simulations

Snow surface temperatures were measured at CDP and WFJ using infrared radiometers. Figure 13 shows scatter plots of hourly observed temperatures against surface temperatures simulated by MSM with parameters for optimal SWE simulations. For WFJ, there is a large scatter in this comparison but the average error is small. The plot for CDP shows two limbs: daily maximum temperatures are simulated quite well, but minimum temperatures at night are much too cold. Because the errors are largest at night, they are insensitive to variations in albedo parameters, and the CDP simulations have already been shown to be rather insensitive to variations in surface roughness. MSM simulations can be greatly improved, however, by the introduction of a "windless exchange coefficient" used in some models to maintain turbulent exchanges between the atmosphere and the surface even in very low windspeed conditions [Jordan et al. 1999, Bruland et al. 2001]: the combination $\rho c_p C_H U_1$ in Eqs (1) and (2) is replaced by $\rho c_p C_H U_1 + V$, where V is a new model parameter. Figure 14a shows how the rms and bias errors in MSM simulations of the CDP surface temperature vary with V; both have low values for $V \approx 2$ $\mathrm{Wm^{-2}K^{-1}}$. Figure 14b shows that both the bias and scatter in the surface temperature simulation are greatly reduced using this value. For comparison, the SNTHERM model uses a value of V $= 1$ $\mathrm{Wm^{-2}K^{-1}}$ by default [Jordan et al. 1999], although higher values have also been used [Rachel Jordan, personal communication].

The increased downward sensible heat flux that increases the surface temperature at night when windless exchange is used for CDP also increases the

snowmelt, giving a poor simulation of SWE. In a previous study using data from Col de Porte, Essery et al. [1999] found that the early melt in simulations with good representations of the surface temperature could be offset by storage of liquid water within the snow. Refreezing of water in the snow also releases latent heat and increases minimum temperatures. These process are not represented in MSM, however, and are not investigated here.

5. Conclusions and Discussion

The accumulation and ablation of snow at four sites was simulated using a simple model with three adjustable parameters that control the radiative and turbulent energy sources for snowmelt. Good simulations of SWE were obtained for each site by adjusting the model parameters. Sensitivity studies showed that the simulations were insensitive to parameter variations in some ranges, but there were also regions of the parameter space that gave very similar simulations for different parameter choices. Because both radiative and turbulent fluxes can contribute energy for snowmelt, it was possible to shift the balance between these energy sources without greatly changing the SWE simulation.

Failures of snow models to predict mid-winter melt events have been noted in previous studies [Slater et al. 2001]. A possible reason for this in models representing snowpacks as a bulk layer is the excess energy required to warm the entire layer to 0°C before melt can begin. Although the simple model neglects heat storage in snow, there are regions of its parameter space in which the significant midwinter ablation observed at one of the sites considered

here is not reproduced; poor parameter choices can lead to poor simulations, regardless of model structure. Removal of snow when the model does not predict melt can also be caused by processes that are not represented, such as wind transport.

Albedo and surface temperature measurements were available for two of the sites. The simple model was able to simulate albedos well, but only at the expense of increasing the rate of snowmelt and giving a poor simulation of SWE. Including a representation of heat fluxes into the snow in an extended version of the model did not improve the best simulations of SWE or albedo attainable individually but gave better simulations of them simultaneously. For a site with low windspeeds, simulated temperatures at night were too low. The temperature simulation was improved by introducing a windless exchange coefficient to maintain turbulent fluxes at low windspeeds, but this again reduced the quality of the SWE simulation. The CROCUS model, which has a much more sophisticated representation of internal snow processes, is able to give much better simultaneous simulations of SWE and surface temperature at this site [Brun et al. 1992, Essery et al. 1999, Etchevers et al. 2004].

Neither MSM nor any of the SnowMIP models explicitly represents blowing snow, but the measured windspeeds at WFJ and GSB frequently exceed typical thresholds of 7 ms^{-1} for transport of dry snow [Li and Pomeroy 1997]. Sublimation of blowing snow may significantly enhance ablation of snow from the surface [Pomeroy and Li 2000]; in a model that does not represent this process, calibration may compensate by selecting an unrealistically large sur-

face roughness. Transport leads to spatial variations in deposition and ablation of snow, so the accumulation at a point on the ground may be either less than or greater than the measured snowfall.

Snow models and land-surface models have increased greatly in sophistication over recent years, and the number of parameters that have to be specified for their operation has increased accordingly. The data available for evaluation of these models is unlikely to contain enough information to determine all these parameters uniquely. Here we found that even the three parameters of a very simple snow model were not tightly constrained by comparison with observations of SWE; indeed, even a temperature index model with a single adjustable melt factor can often provide adequate simulations of SWE [Ohmura 2001]. It has been argued that the use of simpler models with fewer parameters will allow more robust calibration [Franks et al. 1997, Schulz and Beven 2003]. Multiobjective model evaluation may better constrain the parameter calibration [Franks et al. 1999] and may reveal oversimplifications in the model structure. Evaluating the simple snow model in comparison with measurements of albedo and surface temperature (which are closely related to the shortwave and longwave components of the surface energy balance) revealed deficiencies due to the model's neglect of internal snow processes that were not apparent from evaluations of SWE simulations.

Calibrated model parameter values depend not just on the observations to be matched but also on model structure. For comparisons with SWE observations, the fresh snow albedo in MSM is a free parameter that can be adjusted to improve simulations. If a parametrization for albedo decay of

cold snow were included in the model, the optimized values of fresh snow albedo would likely increase. When simulations were compared with measurements of albedo, however, this parameter was directly constrained by the observations.

The observations against which snow models should be evaluated depend on the applications for which they are used. For many hydrological applications, an accurate simulation of the timing and rate of runoff from the snow is sufficient. For avalanche forecasting, however, models have to predict the evolving structure of the snowpack; a comparison of snow profiles predicted by the more sophisticated SnowMIP models with observations is being undertaken [Charles Fierz, personal communication] using the objective method of Lehning et al. [2001]. For atmospheric models, snow models have to supply energy and mass flux boundary conditions. Albedo and surface temperature measurements constrain the radiative fluxes. Although not available for the sites studied here, turbulent fluxes have been measured over snow and used to evaluate models [e.g. Pomeroy and Essery 1999, Box and Steffen 2001, Gustafsson et al. 2001]. There are, however, considerable problems in the measurement of all components of the surface energy balance [Wilson et al. 2002]. A major problem that has still to be adequately resolved is that the length scales on which measurements are available are very different to the scales on which surface models are typically applied. Snowcover is often heterogeneous on scales smaller than the grids used by atmospheric models, and it is hard to obtain accurate SWE data on these scales. One approach to this problem is to use gridded observations or high-resolution models to generate

spatial fields of snow data and use these to evaluate large-scale parametrizations [e.g. Arola and Lettenmaier 1996, Liston et al. 1999].

Evaluations of snow models have often been performed with data collected for other purposes, and the results discussed here highlight some of the problems associated with this. Ideally, models should be evaluated using data from carefully designed experiments. Solid and liquid precipitation should be measured separately close to the area where accumulation on the ground is measured. Sites with minimal redistribution of snow should be chosen unless, of course, models of snow redistribution are to be evaluated. Great care must be taken to ensure that radiometers are kept clear of snow and frost. Uncertainties should be estimated for both evaluation and driving data, and the latter should be translated into uncertainties in model predictions.

Acknowledgements. Meteorological and snow data for this study and SnowMIP were provided by Météo-France (Col de Porte), the Cold Regions Research and Engineering Laboratory (Sleepers River), the Swiss Federal Institute for Snow and Avalanche Research (Weissfluhjoch) and the Meteorological Service of Canada (Goose Bay). Results from SnowMIP models were supplied by the SnowMIP participants: Eric Bazile, Aaron Boone, Ross Brown, Yongjiu Dai, Richard Essery, Pierre Etchevers, Alberto Fernández, Charles Fierz, Yeugeniy Gusev, Rachel Jordan, Victor Koren, Eva Kowalczyk, Yves Lejeune, Eric Martin, Olga Nasonova, David Pyles, Adam Schlosser, Andrey Shmakin, Tanya Smirnova, Ulrich Strasser, Diana Verseghy, Takeshi Yamazaki and Zong-Liang Yang. SnowMIP was supported

by IAHS/ICSI. Richard Essery is supported by NERC advanced research fellowship NER/J/S/2001/00812. Ross Brown, Charles Fierz, Janet Hardy, Andrew Slater and two anonymous reviewers made useful comments on drafts of this paper. This work was influenced by many discussions with John Pomeroy and Danny Marks.

References

Albert, M., and G. Krajeski, A fast, physically based point snowmelt model for use in distributed applications, *Hydrol. Processes*, **12**, 1809–1824, 1998.

Anderson, E.A., Development and testing of snow pack energy balance equations, *Water Resour. Res.*, **4**, 19–37, 1968.

Anderson, E.A., A point energy and mass balance model of a snow cover, *NOAA Tech. Rep. NWS 19*, 150 pp, Off. of Hydrol., Natl Weather Serv., Silver Spring, Md, 1976.

Arola, A., and D.P. Lettenmaier, Effects of subgrid spatial heterogeneity on GCM-scale land surface energy and moisture fluxes. *J. Clim.*, **9**, 1339–1348, 1996.

Barnett, T.P., L. Dümenil, U. Schlese, E. Roeckner and M. Latif, The effect of Eurasian snow cover on regional and global climate variations, *J. Atmos. Sci.*, **46**, 661–685, 1989.

Bartelt, P., and M. Lehning, A physical SNOWPACK model for the Swiss avalanche warning Part I: numerical model, *Cold Reg. Sci. Technol.*, **35**, 123–145, 2002.

Belair, S., R. Brown, J. Mailhot, B. Bilodeau and L.P. Crevier, Operational implementation of the ISBA land surface scheme in the Canadian regional weather forecast model. Part II: Cold season results, *J. Hydromet.*, **4**, 371–386, 2003.

Beven, K.J., and A.M. Binley, The future of distributed models: Model calibration and uncertainty prediction, *Hydrol. Processes*, **6**, 279–298, 1992.

Boone, A., and P. Etchevers, An intercomparison of three snow schemes of varying complexity coupled to the same land surface model: Local-scale evaluation at an Alpine site, *J. Hydromet.*, **2**, 374–394, 2001.

Bowling, L.C., and 23 others, Simulation of high latitude hydrological processes in the Torne-Kalix basin: PILPS Phase 2e. 1: Experiment design and summary intercomparisons, *Global Planet. Change*, **38**, 1–30, 2003.

Box, J.E., and K. Steffen, Sublimation on the Greenland ice sheet from automated weather station observations, *J. Geophys. Res.*, **106**, 33965–33981, 2001.

Brown, R.D., B. Brasnett and D. Robinson, Gridded North American monthly snow depth and snow water equivalent for GCM evaluation, *Atmosphere-Ocean*, **41**, 1–14, 2003.

Brown, R.D., and B.E. Goodison, Interannual variability in reconstructed Canadian snow cover, 1915-1992, *J. Climate*, **9**, 1299–1318, 1996.

Bruland, O., D. Maréchal, K. Sand and A. Killingtveit, Energy and water balance studies of a snow cover during snowmelt period at a high arctic site, *Theor. Appl. Climatol.*, **70**, 53–63, 2001.

Brun, E., P. David, M. Sudul and G. Brunot, A numerical model to simulate snow-cover stratigraphy for operational avalanche forecasting, *J. Glaciol.*, **38**, 13–22, 1992.

Cox, P.M., R.A. Betts, C.B. Bunton, R.L.H. Essery, P.R. Rowntree and J. Smith, The impact of new land surface physics on the GCM simulation of climate and climate sensitivity, *Clim. Dyn.*, **15**, 183–203, 1999.

Desborough, C.E., Surface energy balance complexity in GCM land surface models, *Clim. Dyn.*, **15**, 389–403., 1999.

Douville, H., J.-F. Royer and J.-F. Mahfouf, A new snow parametrization for the Météo-France climate model. I. Validation in stand-alone experiments, *Clim. Dyn.*, **12**, 21–35, 1995.

Dyson, F., A meeting with Enrico Fermi, *Nature*, **427**, 297, 2004.

Essery, R., E. Martin, H. Douville, A. Fernández and E. Brun, A comparison of four snow models using observations from an alpine site, *Clim. Dyn.*, **15**, 583–593, 1999.

Essery, R.L.H., M.J. Best, R.A. Betts, P.M. Cox and C.M. Taylor, Explicit representation of subgrid heterogeneity in a GCM land-surface scheme, *J. Hydromet.*, **4**, 530–543, 2003.

Etchevers, P., and 22 others, Validation of the surface energy budget simulated by several snow models, *Ann. Glaciol.*, **38**, in press, 2004.

Fierz, C., P. Riber, E.E. Adams, A.R. Curran, P.M.B. Föhn, M. Lehning and C. Plüss, Evaluation of snow-surface energy balance models in alpine terrain, *J. Hydrol.*, **282**, 76–94, 2003.

Fierz, C., and M. Lehning, Assessment of the microstructure-based snow-cover model SNOWPACK: thermal and mechanical properties, *Cold Reg. Sci. Technol.*, **33**, 123–131, 2001.

Franks, S.W., K.J. Beven, P.F. Quinn and I.R. Wright, On the sensitivity of soil-vegetation-atmosphere transfer (SVAT) schemes: equifinality and the problem of robust calibration, *Agric. For. Meteorol.*, **86**, 63–75, 1997.

Franks, S.W., K.J. Beven and J.H.C. Gash, Multi-objective conditioning of a simple SVAT model, *Hydrol. Earth System Sci.*, **3**, 477–489, 1999.

Frei, A., and D.A. Robinson, Evaluation of snow extent and its variability in the Atmospheric Model Intercomparison Project, *J. Geophys. Res.*, **103**, 8859–8871, 1998.

Frei, A., J.A. Miller and D.A. Robinson, Improved simulations of snow extent in the second phase of the Atmospheric Model Intercomparison Project (AMIP-2), *J. Geophys. Res.*, **108**, art. no. 4369, 2003.

Goodison, B.E., P.Y.T. Louie and D. Yang, WMO solid precipitation measurement intercomparison: Final report, WMO/CIMO Report 67, WMO/TD 872, World Meteorological Organization, Geneva, 306 pp, 1998.

Gupta, H.V., S. Sorooshian and P.O. Yapo, Toward improved calibration of hydrologic models: Multiple and noncomensurable measures of information, *Water Resour. Res.*, **34**, 751–763, 1998.

Gustafsson, D., M. Stähli and P.-E. Jansson, The surface energy balance of a snow cover: comparing measurements to two different simulation models, *Theor. Appl. Climatol.*, **70**, 81–96, 2001.

Hock, R., Temperature index melt modelling in mountain areas, *J. Hydrol.*, **282**, 104–115, 2003.

Jackson, C., Y.L. Xia, M.K. Sen and P.L. Stoffa, Optimal parameter and uncertainty estimation of a land surface model: A case study using data from Cabauw, Netherlands, *J. Geophys. Res.*, **108**, art. no. 4583, 2003.

Jin, J., X. Gao, Z.-L. Yang, R.C. Bales, S. Sorooshian and R.E. Dickinson, Comparative analyses of physically based snowmelt models for climate simulations, *J. Climate*, **12**, 2643–2657, 1999.

Jordan, R.E., E.L. Andreas and A.P. Makshtas, Heat budget of snow-covered sea ice at North Pole 4, *J. Geophys. Res.*, **104**, 7785–7806, 1999.

Keesman, K.J., Set-theoretic parameter estimation using random scanning and principal component analysis, *Math. Comput. Simul.*, **32**, 535–543, 1990.

Lehning, M., C. Fierz and C. Lundy, An objective snow profile comparison method and its application to SNOWPACK, *Cold Reg. Sci. Technol.*, **33**, 253–261, 2001.

Lehning, M., P. Bartelt, B. Brown and C. Fierz, A physical SNOWPACK model for the Swiss avalanche warning Part III: Meteorological forcing, thin layer formation and evaluation, *Cold Reg. Sci. Technol.*, **35**, 169–184, 2002.

Leplastrier, M., A.J. Pitman, H. Gupta and Y. Xia, Exploring the relationship between complexity and performance in a land surface model using the multicriteria method, *J. Geophys. Res.*, **107**, art. no. 4443, 2002.

Li, L., and J.W. Pomeroy, Estimates of threshold wind speeds for snow transport using meteorological data, *J. Appl. Meteor.*, **36**, 205–213, 1997.

Liston, G.E., R.A. Pielke and E.M. Greene, Improving first-order snow-related deficiencies in a regional climate model. *J. Geophys. Res.*, **104**, 19559–19567, 1999.

Loth, B., and H.F. Graf, Modeling the snow cover in climate studies - 2. The sensitivity to internal snow parameters and interface processes, *J. Geophys. Res.*, **103**, 11329–11340, 1998.

Louis, J.-F., A parametric model of vertical eddy fluxes in the atmosphere, *Bound.-Layer Meteor.*, **17**, 187–202, 1979.

Lynch-Stieglitz, M., The development and validation of a simple snow model for the GISS GCM, *J. Climate*, **7**, 1842–1855, 1994.

Ohmura, A., Physical basis for the temperature-based melt-index method, *J. Appl. Meteor.*, **40**, 753–761, 2001.

Pitman, A.J., Y. Xia, M. Leplastrier and A. Henderson-Sellers, The CHAmeleon Surface Model: description and use with the PILPS phase 2(e) forcing data, *Global Planet. Change*, **38**, 121–135, 2003.

Pomeroy, J.W., and R.L.H. Essery, Turbulent fluxes during blowing snow: field tests of model sublimation predictions, *Hydrol. Processes*, **13**, 2963–2975, 1999.

Pomeroy, J.W., and L. Li, Prairie and Arctic areal snow cover mass balance using a blowing snow model, *J. Geophys. Res.*, **105**, 26619–26634, 2000.

Schulz, K., and K. Beven, Data-supported robust parameterisations in land surface-atmosphere flux predictions: towards a top-down approach, *Hydrol. Processes*, **17**, 2259–2277, 2003.

Sheffield, J., and 14 others, Snow process modeling in the North American Land Data Assimilation System (NLDAS): 1. Evaluation of model-simulated snow cover extent, *J. Geophys. Res.*, **108**, art. no. 8849, 2003.

Slater, A.G., and 33 others, The representation of snow in land surface schemes: results from PILPS 2(d), *J. Hydromet.*, **2**, 7–25, 2001.

Strasser, U., P. Etchevers and Y. Lejeune, Inter-comparison of two snow models with different complexity using data from an alpine site, *Nordic Hydrol.*, **33**, 15–26, 2002.

Sun, S., J. Jin and Y. Xue, A simple snow-atmosphere-soil transfer model, *J. Geophys. Res.*, **104**, 19587–19597, 1999.

Verseghy, D.L., CLASS - a Canadian land-surface scheme for GCMs, *Int. J. Climatol.*, **11**, 111–133., 1991.

Wiesmann, A., C. Fierz and C. Mätzler, Simulation of microwave emission from physically modeled snowpacks, *Ann. Glac.*, **31**, 397–405, 2000.

Wilson, K., and 20 others, Energy balance closure at FLUXNET sites, *Agric. For. Meteorol.*, **113**, 223–243, 2002.

WMO, Intercomparison of models of snowmelt runoff, Operational Hydrology Report 23, World Meteorological Organization, Geneva, 1986.

Xia, Y., A.J. Pittman, H.V. Gupta, M. Leplastrier, A. Henderson-Sellers and L.A. Bastidas, Calibrating a land surface model of varying complexity using multicriteria methods and the Cabauw dataset, *J. Hydromet.*, **3**, 181–194, 2002.

Xue, Y., S.F. Sun, D.S Kahan and Y.J. Jiao, Impact of parameterizations in snow physics and interface processes on the simulation of snow cover

and runoff at several cold region sites, *J. Geophys. Res.*, **108**, art. no. 8859, 2003.

Yeh, T.C., R.T. Wetherald and S. Manabe, The effect of soil moisture on the short term climate and hydrology change - a numerical experiment, *Mon. Wea. Rev.*, **112**, 474–490, 1984.

Tables

	SnowMIP			MSM		
	Minimum	Average	Maximum	Default	Common calibration	Site calibration
CDP	0.24	0.59	1.07	0.41	0.31	0.27
SLR	0.23	0.95	1.90	0.81	0.81	0.24
WFJ	0.20	0.48	1.20	0.31	0.21	0.14
GSB	0.92	2.32	3.59	1.04	0.82	0.56

Table 1. RMS errors in SWE, normalized by the standard deviations of the observations, for SnowMIP models and MSM.

	α	τ (hours)	z_0 (m)
Default	0.85	200	10^{-3}
CDP	0.90	180	1×10^{-3}
SLR	0.96	250	9×10^{-2}
WFJ	0.90	500	3×10^{-2}
GSB	0.98	500	5×10^{-3}
All sites	0.83	500	3×10^{-3}

Table 2. Default and optimized MSM parameters for SWE simulations.

Figure captions

Figure 1. Snow water equivalent, windspeed, air temperature and incoming solar radiation for Col de Porte in 1996-1997. The SWE panel shows cumulative snowfall (line) and accumulation on the ground (diamonds). Shaded bands show periods of ablation.

Figure 2. As Fig. 1, but for Sleepers River in 1996-1997.

Figure 3. As Fig. 1, but for Weissfluhjoch in 1992-1993. Note the change in scale for SWE.

Figure 4. As Fig. 1, but for Goose Bay in 1980-1981.

Figure 5. SWE simulated by MSM with default parameters (dashed lines) and calibrated parameters (solid lines) compared with observations (diamonds). Dotted lines show results for a calibrated degree-day model, and shaded bands show the range of results produced by SnowMIP models.

Figure 6. Normalized errors in SWE simulations (rms errors divided by standard deviation of observations) as parameters (a) α_f, (b) τ and (c) z_0 are varied individually, the other two being fixed at calibrated values given in Table 2. Results are shown for CDP (thick solid line), SLR (dotted line), WFJ (thin solid line) and GSB (dashed line).

Figure 7. Normalized rms errors in MSM simulations of SWE for the SnowMIP sites as model parameters α_f and τ are varied. Regions of the parameter space giving the lowest errors are shaded.

Figure 8. As Fig. 8, but for variations in α_f and z_0.

Figure 9. Measured snow albedo (solid lines) at CDP and WFJ, and MSM

simulations using parameters optimized for SWE simulations (dotted lines) and chosen to minimize rms errors in albedo simulations (dashed lines).

Figure 10. Normalized rms errors in MSM simulations of albedo for CDP and WFJ. Shading shows regions of the parameter space giving the lowest errors in SWE simulations, reproduced from Fig. 7.

Figure 11. As Fig. 10, but for MSM1c simulations.

Figure 12. Pareto curves for CDP and WFJ simulations using MSM (dashed lines) and MSM1c (solid lines).

Figure 13. Surface temperatures simulated by MSM scattered against hourly observed temperatures for CDP and WFJ.

Figure 14. (a) RMS errors (solid line) and bias (dashed line) in MSM simulations of CDP surface temperatures as functions of the windless exchange coefficient V. (b) CDP surface temperatures simulated by MSM with V=2 $\mathrm{Wm^{-2}K^{-1}}$ scattered against hourly observed temperatures.

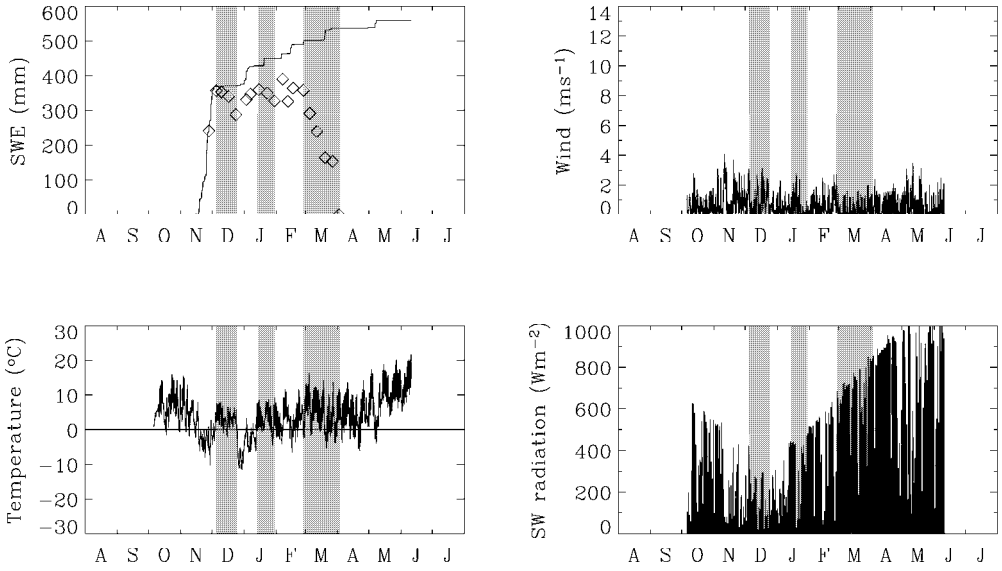

Essery and Etchevers, Figure 1.

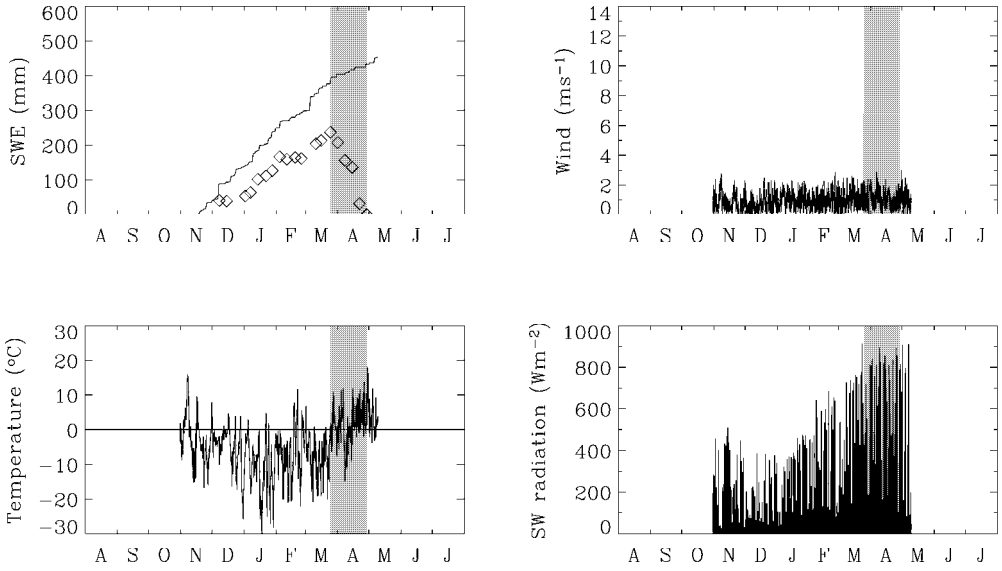

Essery and Etchevers, Figure 2.

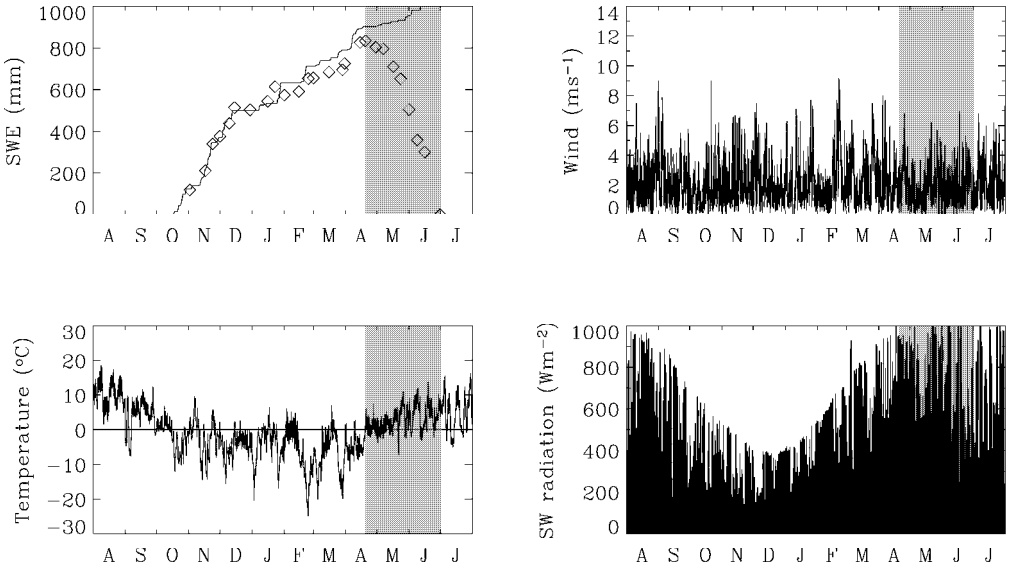

Essery and Etchevers, Figure 3.

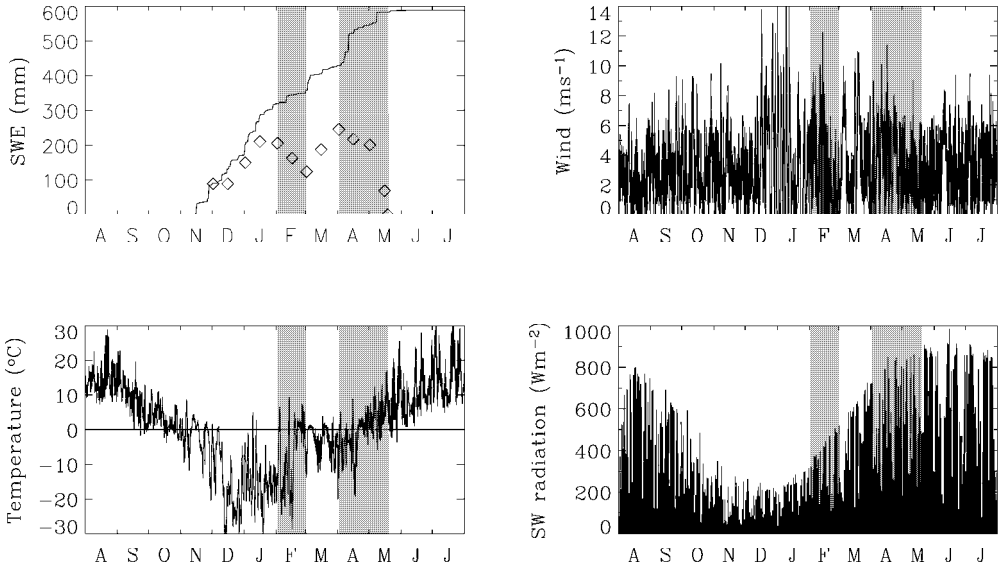

Essery and Etchevers, Figure 4.

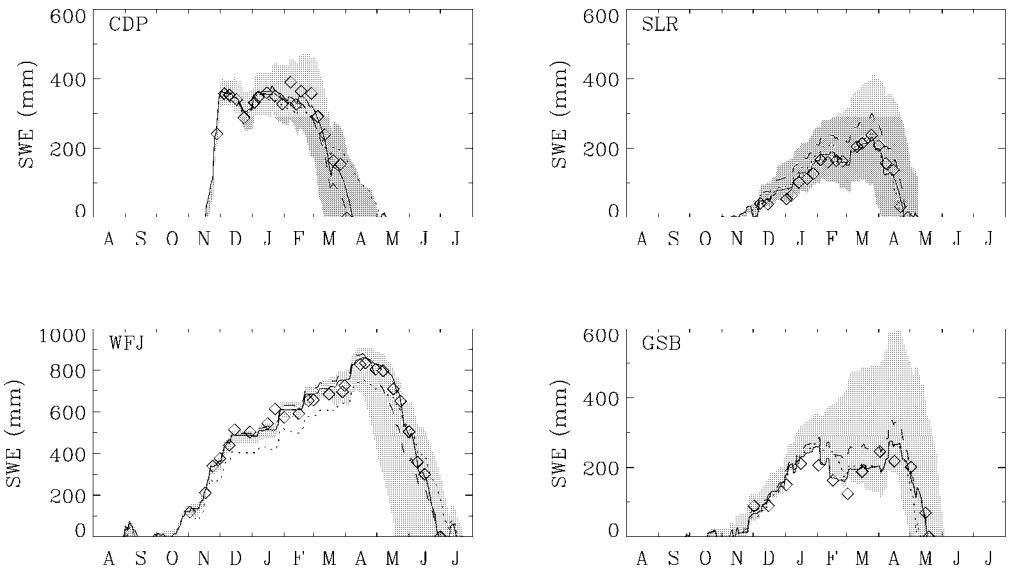

Essery and Etchevers, Figure 5.

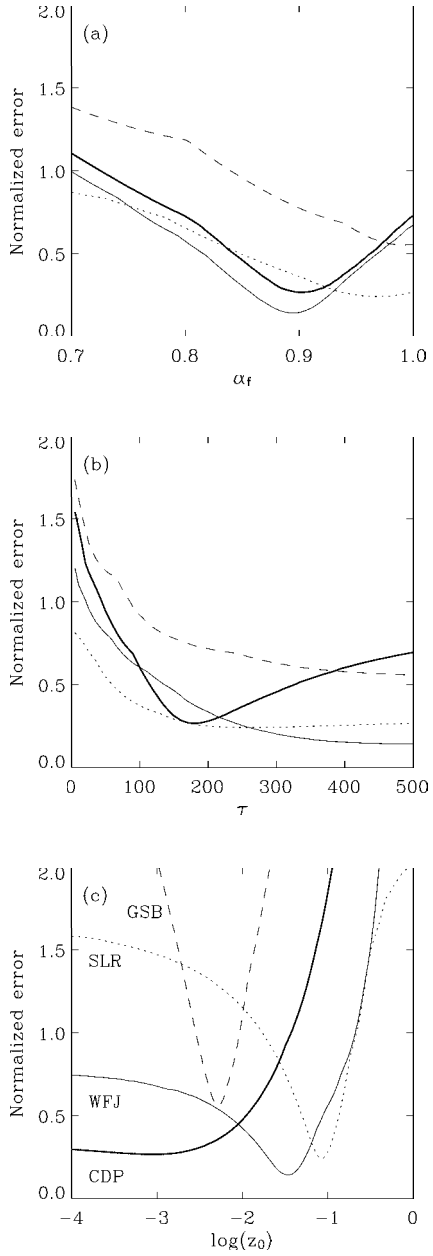

Essery and Etchevers, Figure 6.

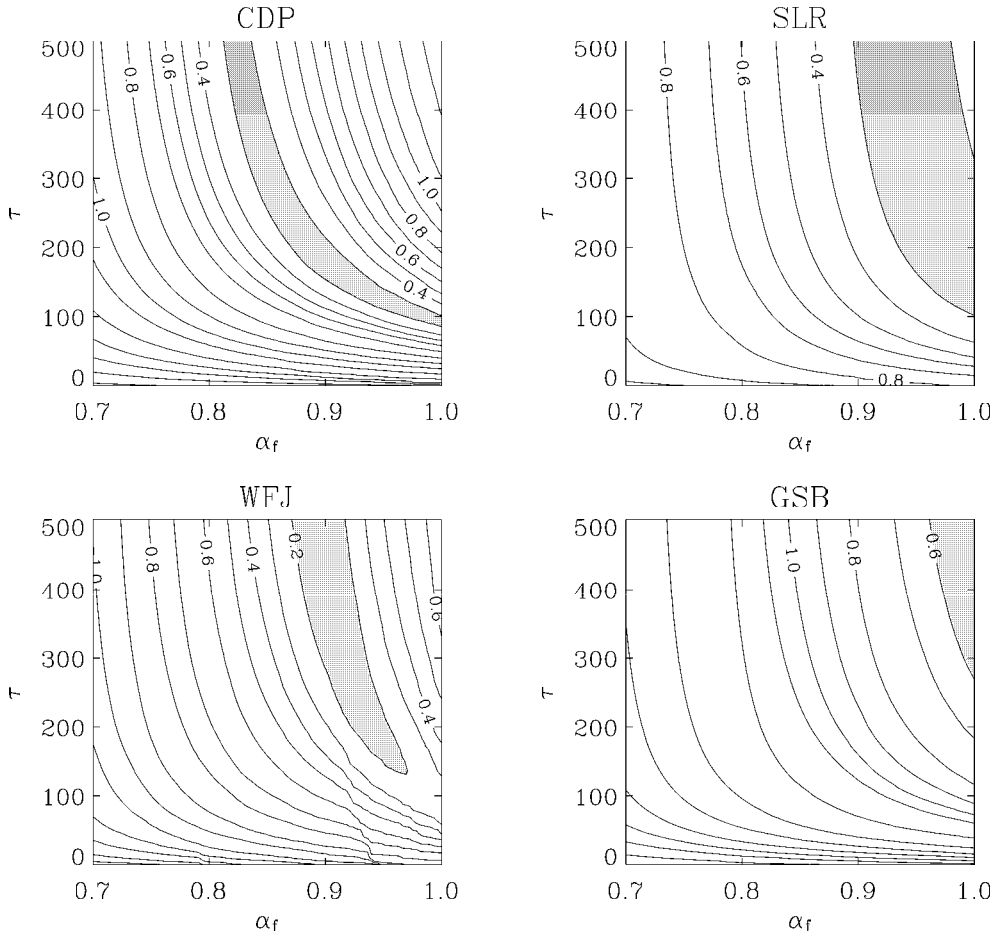

Essery and Etchevers, Figure 7.

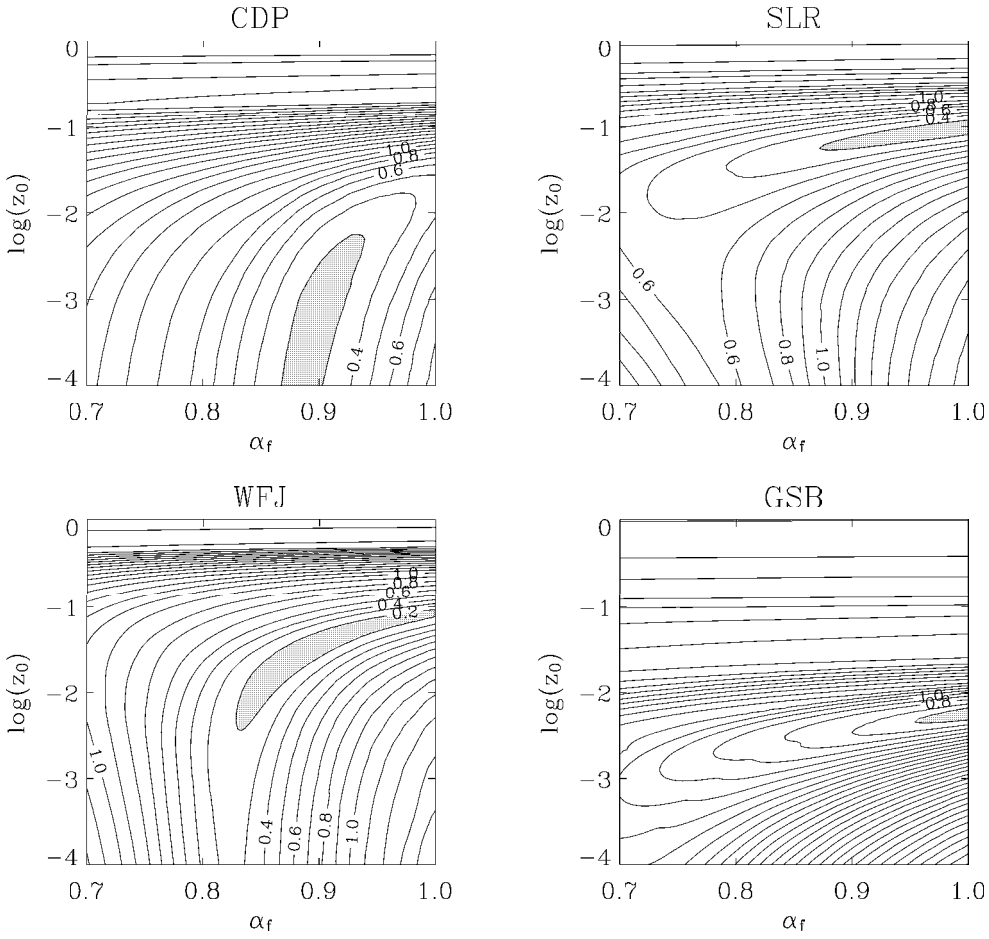

Essery and Etchevers, Figure 8.

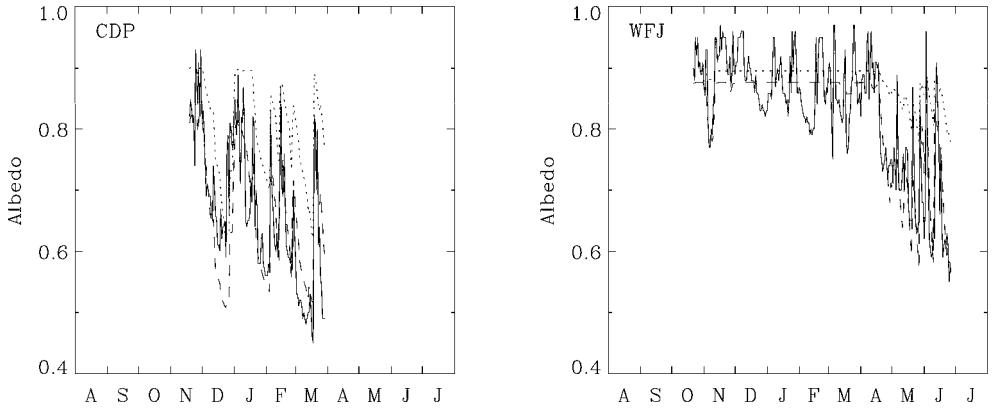

Essery and Etchevers, Figure 9.

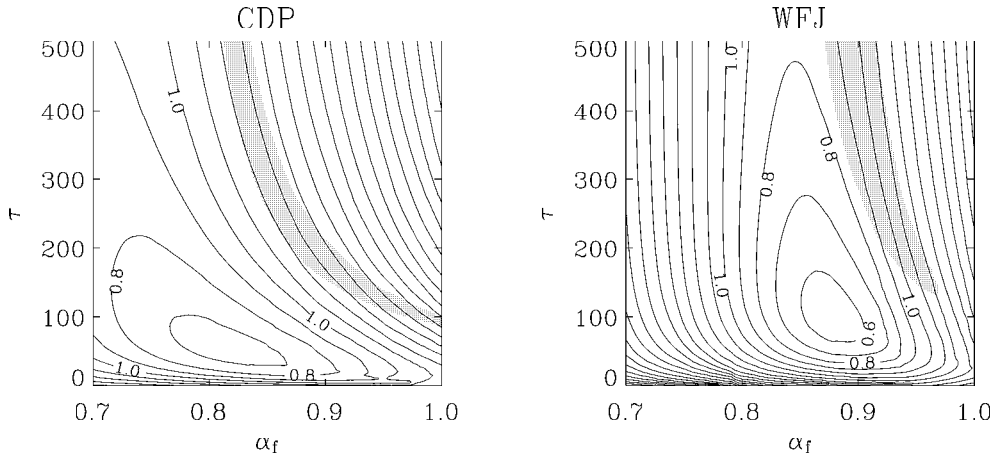

Essery and Etchevers, Figure 10.

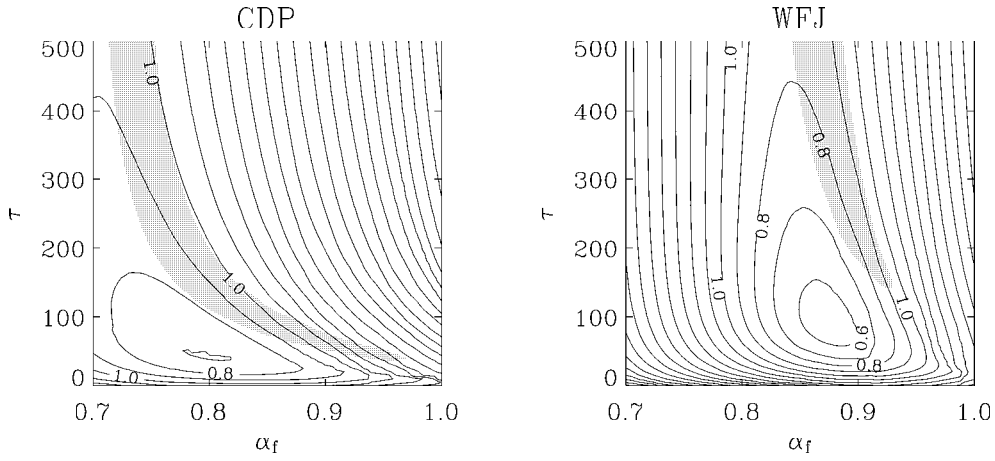

Essery and Etchevers, Figure 11.

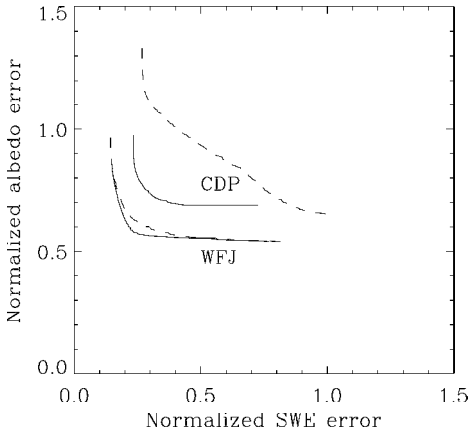

Essery and Etchevers, Figure 12.

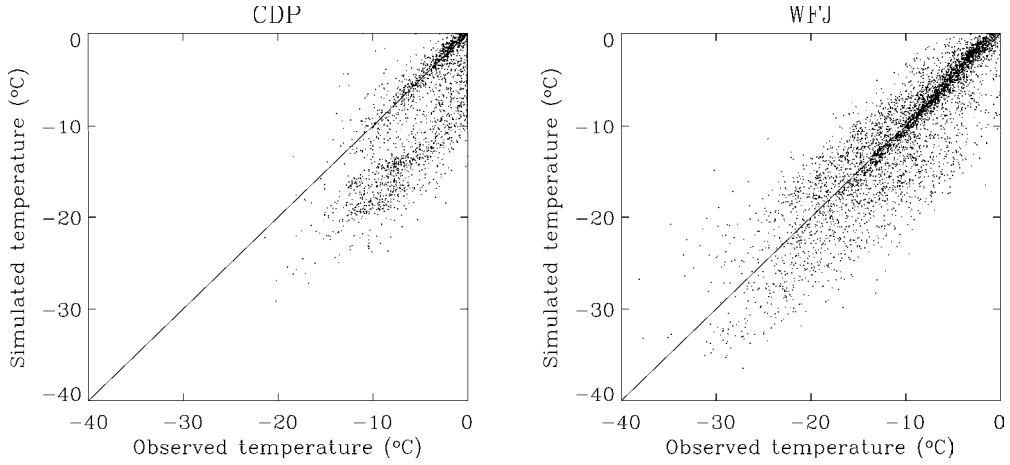

Essery and Etchevers, Figure 13.

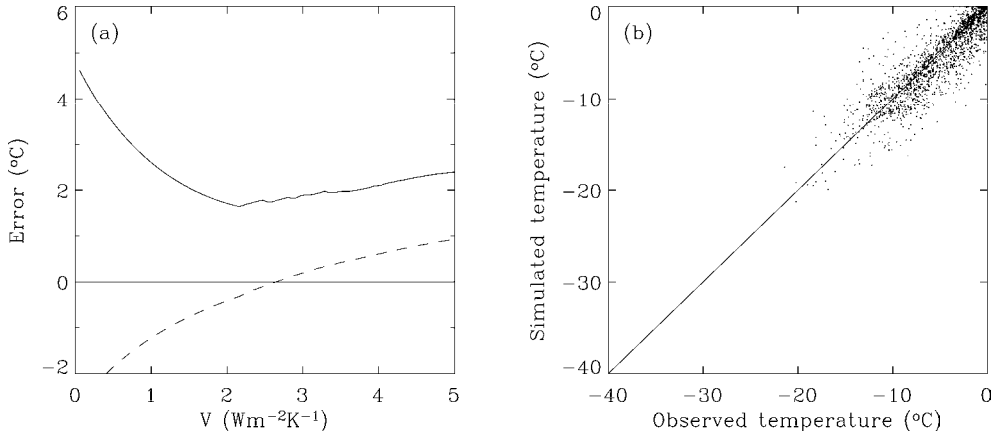

Essery and Etchevers, Figure 14.